

Integrated Characterization and Forecasting of Overpressure Mechanisms in the 'Nge' Field, Offshore Niger Delta: Insights from Rock Properties - Seismic Velocity Cross-Plot Analysis

*¹Ideozu, R. U, ²Mba-Otike, M. N and ³Odumoso, S. E

¹Department of Geology University of Port Harcourt

²Department of Geology, Dennis Osadebay University Delta State

³Department of Earth Sciences Federal University of Petroleum Resources, Effurun, Delta State

*Corresponding Author

DOI: <https://doi.org/10.51244/IJRSI.2025.12010048>

Received: 04 January 2025; Accepted: 08 January 2025; Published: 12 February 2025

ABSTRACT

The overpressure mechanisms in the NGE Field, located offshore in the Niger Delta, were investigated using a cross-plot analysis of rock properties and seismic velocities. Overpressure, which is primarily caused by disequilibrium compaction and unloading mechanisms, poses significant challenges during hydrocarbon exploration and drilling operations in the region. Wireline log data (sonic, density, resistivity, and gamma-ray logs) and 3D seismic data were employed to delineate overpressure zones and estimate their magnitudes using Eaton's and Bowers' methods. These data sources collectively provide critical insights into pore pressure, compaction, fluid saturation, lithology, and structural context, which are essential for accurate delineation of overpressure zones. Three distinct overpressure zones A, B and C were identified across the NGE X, Y, and Z wells, with depths ranging from 7,600 to 12,700 feet. The primary cause of overpressure in zones A and B is disequilibrium compaction, indicated by deviations from the normal velocity trend, with pressure values slightly above normal levels, typically around 0.5 to 1.0 psi/ft. In contrast, unloading due to tectonic stress is responsible for the high overpressure in zone C, where pressures can exceed 1.5 psi/ft. The results demonstrate that faults, particularly major growth faults in the region, played a critical role in overpressure development, with wells drilled across fault planes exhibiting higher overpressure magnitudes. The need for integrating seismic and well log data for accurate pore pressure prediction is therefore emphasized in this study, highlighting the importance of understanding overpressure mechanisms for safer and more efficient hydrocarbon exploration in the complex geological settings of the Niger Delta.

Key Words: Over Pressure Mechanisms, Forecasting Over pressure, Rock Properties, Seismic Velocities

INTRODUCTION

Hydrocarbon-bearing basins worldwide are often associated with at least one pressure regime, having significant impact on exploration and exploitation of the resource (Wang, 2016 and Ganguli and Sen, 2020). Normal, overburden and formation or pore pressures are the three basic types of pressure that exist in hydrocarbon reservoirs. Formation or pore pressure is the pressure exerted by fluids within the pore spaces of rock formations. Pore pressure is known to be related to a host of geological processes such as tectonics, fluid expansion, lateral transfer disequilibrium compaction, etc. But the Niger Delta basin is mostly associated with disequilibrium compaction of shales (Swarbrick and Osborne, 1998; Gutierrez *et al.*, 2006; Olatunbosun, 2014; Eze *et al.*, 2018). This pressure can vary significantly depending on geological conditions and can be classified as normal, abnormal (overpressure), or subnormal (Fertl, 1981; Bjørlykke and Høeg, 1997; Harold, 2001; Godwin, 2013; Hamid, 2013; Rezaee, 2015; Atashbari, 2016; Olorunfemi, 2019; Zhang *et al.*, 2020; Abbey *et al.*, 2020; Eyinla *et al.*, 2021; Nwonodi and Dosunmu, 2021 and Birchall *et al.*, 2022).

Normal formation pressure aligns with hydrostatic conditions, while overpressure or abnormal formation pressure exceeds hydrostatic levels, often requiring additional measures during drilling to manage potential influxes of formation fluids. Overpressure in sedimentary formations can arise from several geological activities, including compaction disequilibrium, hydrocarbon generation, gas cracking, aqua-thermal expansion, and tectonic compression (De Souza, 2020 and Li *et al.*, 2022).. Subnormal formation pressures on the other hand, are those that fall below hydrostatic levels, typically resulting from geological changes such as uplift or fluid extraction (Louden, 1972 and Barker, 1987). Among these pressure regimes, overpressure (high abnormal formation pore pressures) poses considerable operational risks during drilling operations (Carvajal and Sierra, 2020; Akrouit *et al.*, 2021 and Ovwigho *et al.*, 2023). Understanding the mechanisms behind overpressure is crucial, particularly in highly prolific basins like the Niger Delta (Odesa *et al.*, 2024), which is characterized by complex geological processes that contribute to abnormal pressure conditions.

The Abnormal pressure conditions are categorized into three primary mechanisms: loading, unloading, and tectonic stress. The loading mechanism relates exclusively to reservoir conditions, where rapid sedimentation confines pore fluids within the formation, leading to increased pore pressure. Conversely, unloading mechanisms result from fluid expansion or erosional uplift that rapidly increases pore pressure by releasing confined sediments. Tectonic stress mechanisms occur in zones where fluid expulsion cannot keep pace with rapid increases in tectonic stress (Swarbrick and Osborne, 1998; Shunhua *et al.*, 2006; Gutierrez *et al.*, 2006; and Alias, 2011).

In the Niger Delta Basin, geological conditions favour the development of overpressure zones primarily due to disequilibrium, compaction and unloading effects. The region's young geological age and predominant shale lithology make it particularly susceptible to these overpressure mechanisms (Zhang *et al.*, 2021 and Alao *et al.*, 2014). Accurate prediction of overpressure relies on understanding compaction-dependent geophysical properties such as sonic velocities and density measurements. Shales are particularly responsive to overpressure changes, making them critical for pore pressure prediction (Mavatikua, 2005; Oloruntobi, 2019 and Unuagba *et al.*, 2021)

The significance of accurately predicting and estimating overpressure cannot be overstated. Catastrophic incidents like kicks, blowouts, environmental pollution, and loss of life can occur if these pressures are not adequately assessed before drilling (Alao, 2014; Eze *et al.*, 2018). This study aims to mitigate these risks by employing well logs and seismic data to predict and estimate overpressures in the NGE Field of the Niger Delta. By identifying overpressure zones and estimating their magnitudes, this study contributes to safer exploration practices in a region known for its complex pressure dynamics.

This study also attempts to delineate overpressure zones within the NGE Field and estimate their magnitudes using advanced analytical techniques. Specific objectives employed to achieve this aim include predicting overpressure through analysis of Overburden and Normal Compaction Trends (NCT) derived from density and sonic logs; applying Eaton's and Bowers' equations for pressure estimation; delineating under-compaction and unloading trends through cross-plot analysis of velocity and density; and conducting a structural interpretation of seismic data to assess the influence of tectonic stress mechanisms.

While existing methodologies for pore pressure prediction using wireline and seismic data have proven valuable, they often lack the depth required for comprehensive analysis. This study seeks to enhance these methodologies by estimating overpressures at various depth intervals, thus providing a more thorough understanding of pressure dynamics, improving the accuracy of pore pressure predictions, ultimately enhancing safety and efficiency in hydrocarbon exploration activities.

The Niger Delta Basin, located between latitudes 3° and 6° N and longitudes 5° and 8° E (Figure 1), occupies a significant part of the Gulf of Guinea continental margin in equatorial West Africa (Haack *et al.*, 2000; Doust, 1990; Adegoke *et al.*, 2017 and Odesa *et al.*, 2024). Covering an area of approximately 75,000 km², this basin represents about 7.5% of Nigeria's landmass and is characterized by a low-lying floodplain that developed over an older transgressive Paleocene prodelta. It is the youngest and southernmost of three large sediment bodies formed following the separation of the African and South American plates (Ajakaiye and Bally, 2002; Adegoke *et al.*, 2017; Dim and Dim, 2021; Chukwu and Obiora, 2021 and Akpa *et al.*, 2023). The Niger Delta,

which is on the passive western margin of Africa, is one of the largest modern deltaic systems in the world. The Delta is an arcuate, wave- and tide-influenced progradational complex. The Dahomey Basin borders it to the west; the Abakaliki Fold Belt and Calabar Flank are at the eastern margins of the basin, while its northern and southern limits are the Anambra Basin and the Gulf of Guinea respectively (Figure 2)

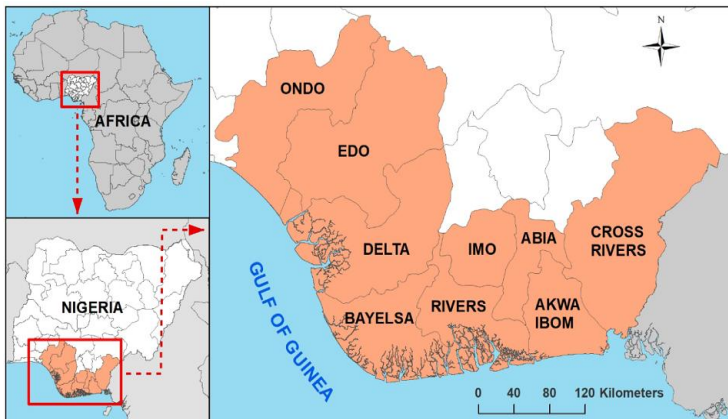


Fig.1. Map of the Niger Delta region (NDR) of Nigeria (Source: Odesa *et al.*, 2024)

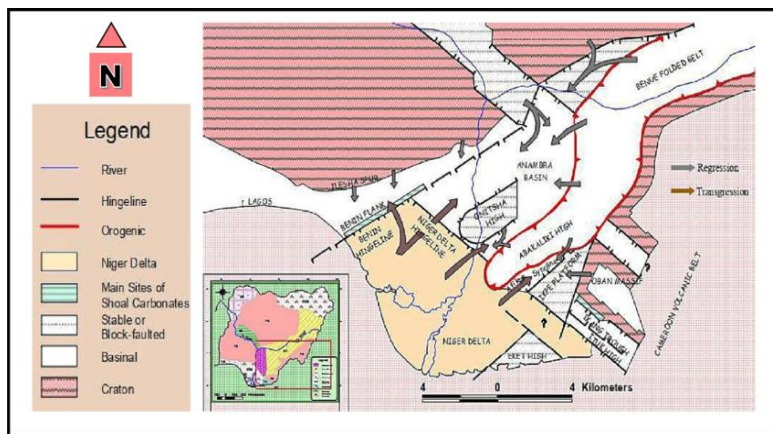


Fig. 2. Tectonic map showing the Niger Delta (modified after Kogbe, 1989)

The stratigraphy of the Niger Delta is divided into three major lithostratigraphic units: The Akata Agbada and Benin Formations (Table 1; Fig. 3). Akata Formation consists of predominantly marine shales deposited during the Palaeocene to Recent and serves as the primary source rock for hydrocarbons in the region, characterized by dark grey sandy silt shale with organic-rich layers at its uppermost sections (Short and Stauble, 1967). The Akata Formation typically exceeds 4,000 feet in thickness and is known for its uniform shale development. Agbada Formation: Overlying the Akata Formation, the Agbada Formation is a complex sequence of fluvio-marine sands intercalated with shales. The formation is Eocene to Recent and can reach thicknesses of over 10,000 feet. The Agbada Formation contains significant hydrocarbon reservoirs within its sandy units, often enclosed by structural traps such as rollover anticlines formed during sedimentary deformation (Ogbamikhumi and Igbinigie, 2020).

The Benin Formation on the other hand is the uppermost unit, and consists of continental deposits characterized by massive sandstones with intercalated shales. This formation is predominantly composed of fresh water-bearing sands and gravel deposited in an upper deltaic plain environment. The thickness exceeds 6,000 feet but has limited hydrocarbon accumulation compared to the underlying formations (Kogbe, 1976). The Niger Delta Basin is an extensional rift basin that formed during the late Jurassic to mid-Cretaceous period due to tectonic activities associated with the breakup of the African and South American plates (Haack *et al.*, 2000). This geological evolution has resulted in a structurally complex basin characterized by high-angle normal faults and shale diapirism caused by loading from overlying sediments (Luo, 2004 and Suppe, 2014). The basin's tectonic structure can be divided into several zones: an extensional zone on the continental shelf, a transition zone, and a contraction zone in deeper waters.

Table 1: Formations of the Niger Delta Area and their relative age (After Short and Stauble, 1967)

SUBSURFACE			SURFACE OUTCROPS		
Youngest Known Age	Formation	Oldest Known Age	Youngest Known Age	Formation	Oldest Known Age
Recent (Short and Stauble, 1967)	Benin Formation	Oligocene (Obaje and Amajor, 2000)	Pleistocene (Ojo and Rahaman, 1989)	Benin Formation	Oligocene (Obaje and Amajor, 2000)
Pliocene (Dewey and Wolela, 1972)	Agbada Formation	Eocene (Kogbe, 1978)	Miocene (Dixon, 1964)	Ogwashi Asaba Formation	Oligocene (Nwajide, 1990)
			Middle Eocene (Obaje, 2009)	Ameki Formation	Early Eocene (Avbovbo, 1978)
Miocene (Petters, 1982)	Akata Formation	Palaeocene (Wright, 1985)	Early Eocene (Kogbe 1976)	Imo Shale	Late Cretaceous (Wright, 1985)

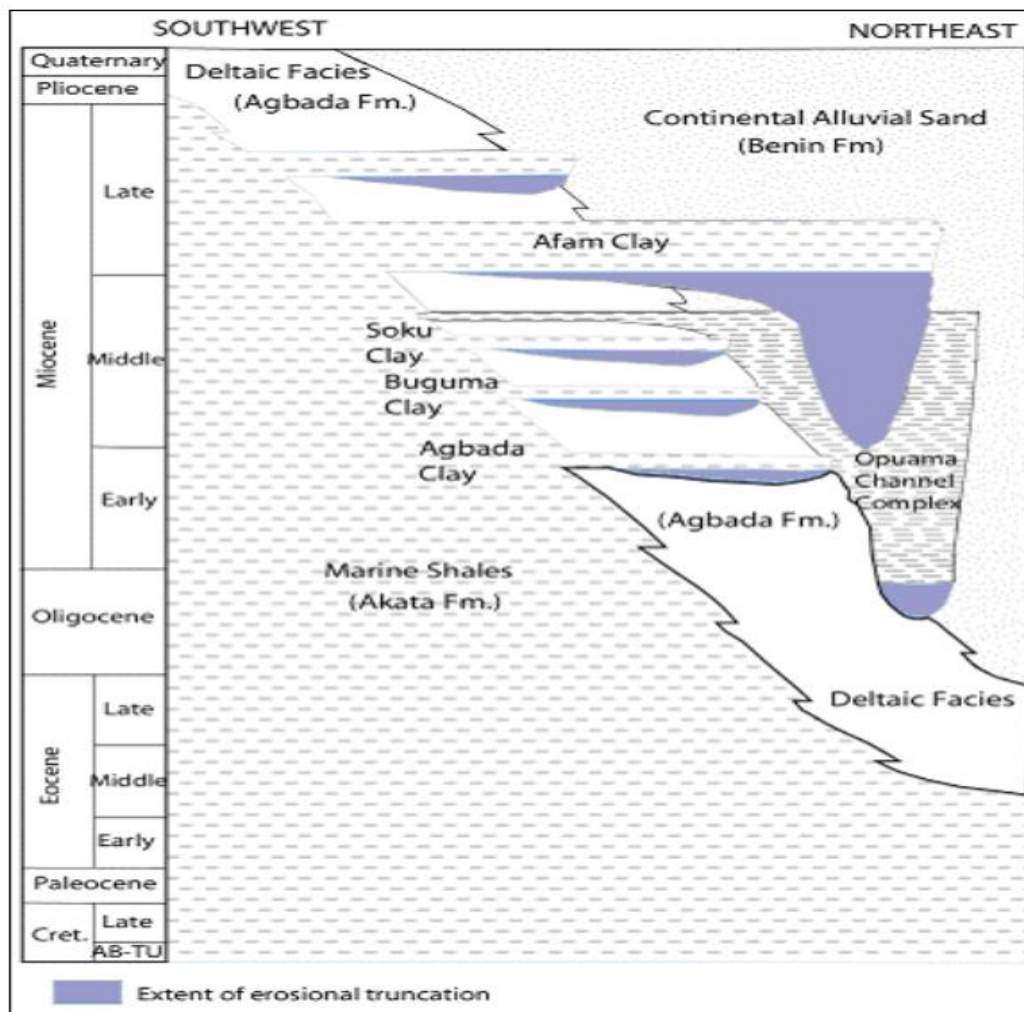


Figure 3. Stratigraphic datasheet showing the three Formations of the Niger Delta. (Aminu and Olorunniwo, 2012).

The interplay between sedimentation processes and tectonic forces has led to unique features such as basinward dipping reflectors and shale diapirs originating from the Akata Formation. These structures play a crucial role in hydrocarbon trapping mechanisms within the basin (Doust and Omatsola, 1990). Additionally, episodes of structural collapse have influenced sediment transport patterns, leading to significant variations in lithology across different depositional environments within the delta (Abam and Omuso, 2000 and Busari and Adekeye, 2024). Understanding the stratigraphy and geological setting of this basin is essential for effective hydrocarbon exploration strategies.

MATERIALS AND METHODS

The dataset utilized in this study comprised wireline log data, including sonic, density, resistivity, and gamma ray logs, alongside three-dimensional seismic data in SegY format and check shot data. Prior to analysis, the data underwent a meticulous organization and cleaning process using Microsoft Notepad and Excel to rectify any errors, such as negative values. The seismic data were subsequently processed in Petrel to enhance various attributes, notably faults and horizons.

For data importation, wireline data were integrated into Rokdoc, while the three-dimensional seismic data were loaded into Petrel. This comprehensive dataset included geographical locations, well headers, and well deviation information. Faults within the geological structure were identified based on reflection discontinuities and other seismic anomalies. A compressional velocity (V_p) log model was constructed and calibrated with check shot data to generate synthetic seismograms. This model was crucial for facilitating the tie between the seismic data and well logs.

In predicting pore pressure from well logs, overpressure was estimated using sonic and density logs through velocity reversals and effective stress trends. The effective stress (σ') can be expressed as:

$$\sigma' = \sigma - P_p$$

Where σ is the total stress and P_p is the pore pressure.

Terzaghi's Method (1943) relates overburden stress to pore and effective stresses for estimating overpressure. This method is based on the principle that the pore pressure increases as the effective stress decreases due to the weight of the overburden. The equation can be represented as follows:

$$P_p = (k * \sigma) - \sigma'$$

Eaton's Method (1975) utilizes sonic velocity to predict overpressure by analyzing deviations from standard compaction trends. This method assumes that the sonic velocity decreases with increasing pore pressure, allowing for the estimation of overpressure based on the measured sonic velocities. The equation is given as:

$$P_p = (V_n - V_s) / (V_n - V_p)$$

Bowers' Method (1995) amalgamates unloading, under-compaction, and normal compaction into a singular equation for estimating pore pressure based on compressional velocity (V_p) and effective stress (σ). This method provides a more comprehensive approach by considering the effects of both unloading and under-compaction. The equation can be represented as:

$$P_p = (C * V_p) - \sigma'$$

Each method was systematically applied to estimate pore pressure within the studied formation, yielding valuable insights into zones of overpressure.

The pressure cell method was employed to differentiate pressures in sand and shale formations, leading to the creation of a two-dimensional overburden trend model that illustrated effective stress variations. Key

indicators of overpressure included noticeable changes in colour contrasts of pressure cells, shifts in density trends, and deviations from expected effective stress values. The relationship between pore pressure and compaction was examined through compressional velocity (V_p), density, and porosity logs; deviations from normal compaction trends indicated instances of overpressure resulting from either under-compaction or unloading mechanisms. Unloading was characterized by diminished grain contact stress alongside reduced velocity without further loss of porosity.

RESULTS AND DISCUSSIONS

The results of this study are presented in terms of velocity determination for overpressure estimation, normal compaction trend of the shale zone and top of the overpressure zone and cross-plots of rock properties of the overpressure zones. The result of overpressure prediction from velocity determination of Wells X to Z in NGE Field is presented in Figures 4(a-c). Three overpressure zones (top – bottom pressure range) were identified in well NGE X based on reduced velocity signatures from the normal velocity travel trend (Figure 4a). The overpressured zones were designated as; A (7600ft – 8800ft), B (9200ft – 10100ft) and C (10500ft – 11000ft) (Table 2). Under-compaction (disequilibrium compaction) is believed to be the cause of overpressure in A and B because the velocity trend slightly deflected away from the normal compaction trend in the depths of overpressure zones aforementioned. At C, there was a sharp deflection from the normal compaction trend and the magnitude of deflection in Figure 5a was larger than the deflections in overpressure zones A and B, thus the cause of overpressure may be related to unloading. Further proof can be seen when shale density from the overburden trend in Figure 4(a-c) is abnormally reduced and remains static at the same depth. The identification of the cause of overpressure across the wells was based on Chopra and Huffman (2006) identification technique. were slight reduction of velocity signatures at 8100ft – 8500ft, 8700ft – 9700ft and 10300ft – 11000ft respectively which represents the only over pressure zones existent in this well and it was designated as A, B and C. The magnitude of decrease in velocity from the normal travel trend is relatively low in A and B when compared to C in Figure 4b. Invariably overpressure magnitudes in A and B are just slightly above normal pressure in overpressured zones (A and B). Disequilibrium compaction (under-compaction) is identified as the cause of overpressure in NGE Y based on Chopra and Huffman, 2006 techniques. In NGE Z well, three overpressured zones were identified, they are A (8000ft – 9000ft), B (10000ft – 10500ft) and C (11800ft – 12700ft) (Figure 4c, Table 2). Velocity signature slightly deviated away from the normal travel trend in overpressure zone A, which indicates mild overpressure. In overpressure zone B, there was significant deflection of velocity signatures away from the normal travel trend, while in overpressure zone C, the velocity deflection from the normal travel trend was steep and at this depth also, shale density remained constant in the overburden trend in Figure 4. The steep velocity deflection indicates high overpressures and when combined with the density scenario it can be deduced that the cause of overpressure points to unloading (Chopra and Huffman, 2006). The normal compaction trend for each well was derived from the compressional (V_p) sonic velocity logs as presented in Figure 5 (a-c). Significant deviations from the normal compaction trend, suggests the onset of overpressure in a well. Three Tops of overpressure (TOV1, TOV2 and TOV3) identified from wireline logs of Wells NGE X – Z and the over-pressured tops across the wells were correlated (Figure 6). Overpressure tops for NGE X occurred at depths of 7600ft, 9200ft and 10500ft, for NGE Y well the overpressure tops occurred at depth of 8100ft, 8700ft and 10300ft, whereas the overpressure tops for NGE Z occurred at depths of 8000ft, 10000ft and 11800ft respectively (Figures 5a and 5c). The results of loading and unloading determined from cross-plots of the studied wells is presented in Figure 7 (a, b and c). Loading events consists of continuous increase of the overburden stress. It is identified on velocity – density cross plot by slow but continuous increase in effective stress, density and velocity (Figure 7b). In unloading events, compaction is brought to a halt (Chopra and Huffman, 2006) and it is identified by sharp velocity reversal and abrupt stand still of density i.e. density stops increasing because the load is either carried entirely by the pore fluids or uplifts must have occurred (Figure 7a and c). Thirteen faults (1-13) were identified across the seismic section (Fig 8; Table 3), three of which are major faults (1, 9 and 11) and the rest minor faults. The fault type in the NGE field is interpreted as growth faults typical of the Niger Delta (Opara and Onuoha, 2009) which is believed to have contributed to the high overpressures at depth in this field. Fault planes act as potential seals for hydrocarbons (Opara and Onuoha, 2009), thus NGE X and Z were spudded across faults 8 and 9 (minor and major faults) respectively to get the hydrocarbon bearing zones. From overpressure analysis carried out in the wells, it was observed that wells spudded across fault lines in NGE Field had high overpressure magnitudes

especially at the area where it cuts across the fault plane thus, if properly managed, would boost production. Overpressure analysis in NGE field shows that under-compaction (loading) mechanism of overpressure, characterized by gradually, increasing mild overpressure with depth in the areas of interest (Chopra and Huffman, 2006), is the main cause of overpressure in zones A and B across the three wells including zone C of NGE Y.

Table 2: Identified overpressure zones and range of estimates of overpressure in wells NGE X, NGE Y and NGE Z from Eaton and Bowers methods

Well	Overpressure Zone	Overpressure Estimates from Eaton's Method (Psi)	Overpressure Estimates from Bowers Method (Psi)
NGE X	A TOV1 (7600 -8800ft)	4121.6 – 5540.5	3648.6 – 5747.3
NGE X	B TOV2 (9200 – 10100ft)	5405.4 – 6175.7	5472.9 – 6229.7
NGE X	C TOV3 (10500 – 11000ft)	7162.2 – 7891.9	7229.7 – 7972.9
NGE Y	A TOV1 (8100 – 8500ft)	3942.3 – 4615.4	4038.5 – 4807.7
NGE Y	B TOV2 (8700 – 9700ft)	4423.1 – 5480.8	4519.2 – 5528.8
NGE Y	C TOV3 (10300 – 11000ft)	5673.1 – 6923.1	5557.7 – 6826.9
NGE Z	A TOV1 (8000 – 9000ft)	3576.5 – 4705.9	3676.5 – 4779.4
NGE Z	B TOV2 (10000 – 10500ft)	5073.5 – 5882.3	5235.3 – 6323.5
NGE Z	C TOV3 (11800 – 12700ft)	6470.6 – 8676.5	6176.5 – 7926.5

Velocity travel trend increased normally with depth in NGE Y (Figure 4b, Table 2), however in addition, unloading from tectonic activities is believed to have induced overpressures in zone C in NGE X and Z respectively. The pressure values in zone C of NGE X and Z were extremely high and it is believed to have been induced by tectonic uplifts in the hanging walls of Faults 8 and 9 which aligns with Opara and Onuoha, (2009), which unloaded the weight on the underlying sediments in the footwall, thus causing massive pressure romps in the footwall where the overpressure zone C of NGE X and Z were located respectively (Fig. 9). Although pressure readings in NGE X and Z are significantly high, NGE Z readings were slightly higher because it was drilled across a major fault (9) while its counterpart was drilled on a minor fault (8). From this finding the major faults blocks have higher displacements in comparison to the minor faults that created unloading scenarios in a typical roll-over or anticlinal structure. It is important to note that there were no pressure romps in NGE Y, because it was not drilled across a fault line (Figure 9). Secondly, the entire overpressure in this field was governed by undercompaction (as it can be seen in Overpressure zones A and B across the wells in Figures 4, 5 and 6) and this type of overpressure mechanism cannot yield massive overpressure at average depths according to Bowers (2002), but this pressure can continue to build-up with increasing depth, hence it can increase to the point where it can stop compaction process if the rock matrix does not crack to bleed off this pressure. Overpressure zones A, B and C for the three wells were correlated separately using Microsoft excel scatter plots (Figures 10 and 11). From the separate correlations, overpressures and its normal pressure readings were plotted with depth to delineate the distance between the normal pressures and the supposed overpressure. In all the zones influenced by undercompaction (overpressure zone A, B across the three wells and C of NGE Y), NGE X has the highest magnitude of overpressure followed by NGE Z and NGE Y. In overpressure zone C of NGE X and Z, the overpressure magnitudes in NGE Z were higher than those in NGE X.

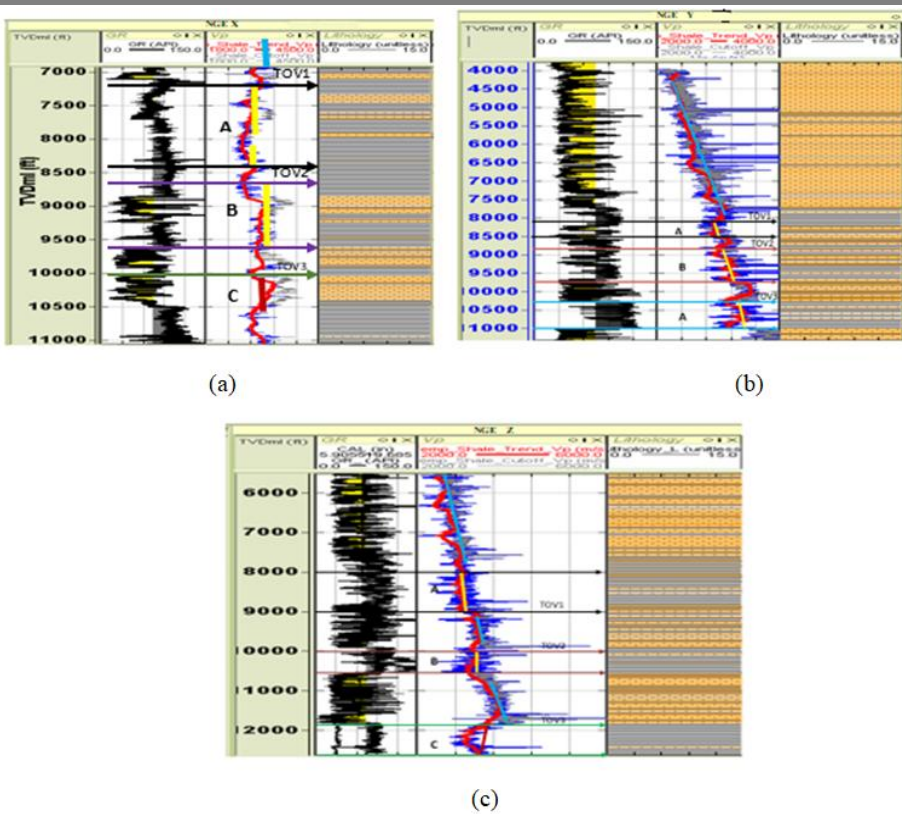


Figure 4. Velocity and Gamma ray logs showing top of overpressure (TOV1 - TOV3), overpressure zones (A, B and C) and rock physical properties of normal compaction (blue trend line), disequilibrium compaction/under-compaction (yellow trend line) and Unloading (red trend line) for NGE X, Y and Z (a) NGE X, (b) NGE Y, (c) NGE Z (Rokdoc software, 2010 version).

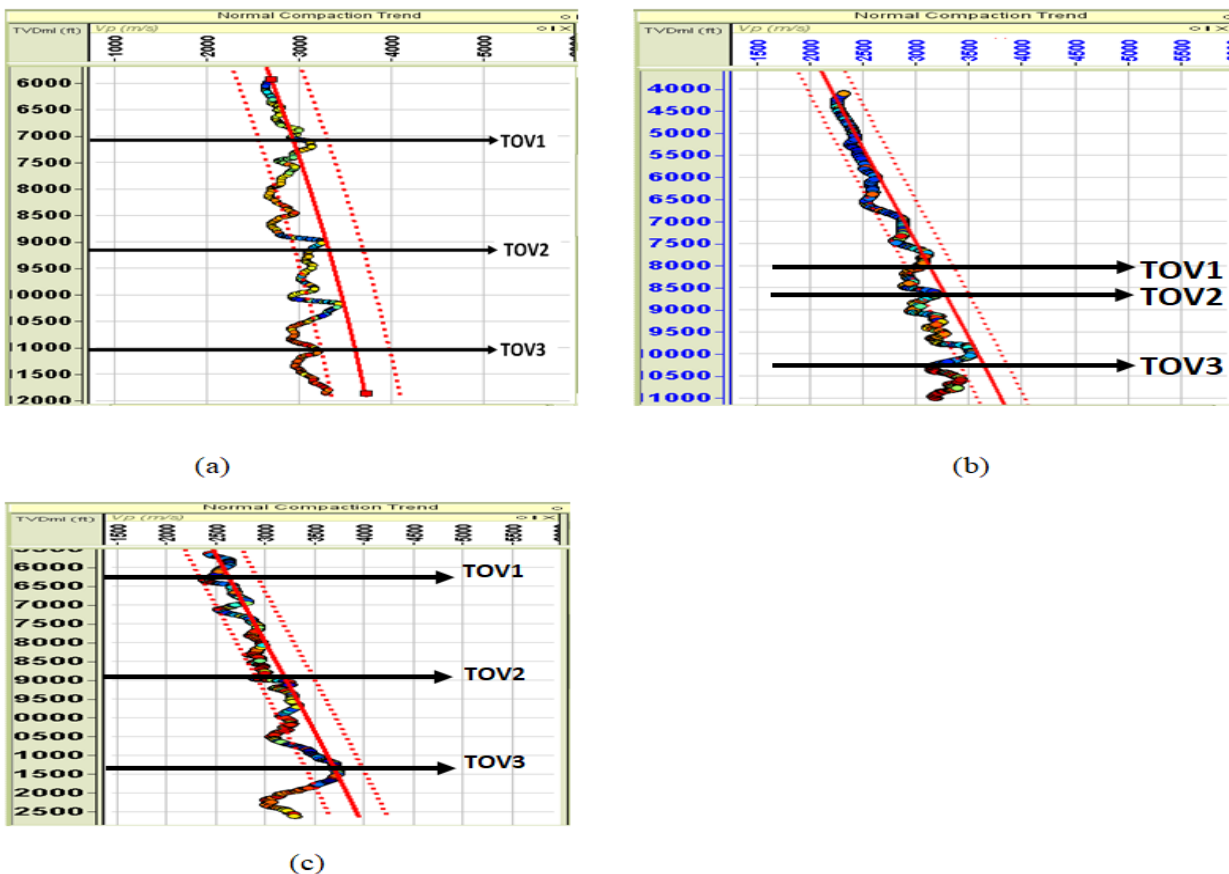


Figure 5 Normal compaction trend (NCT) from Compressional sonic velocity (Vp) log of NGE X – Z, (a) NGE X, (b) NGE Y, (c) NGE Z (Rokdoc software, 2010 version)

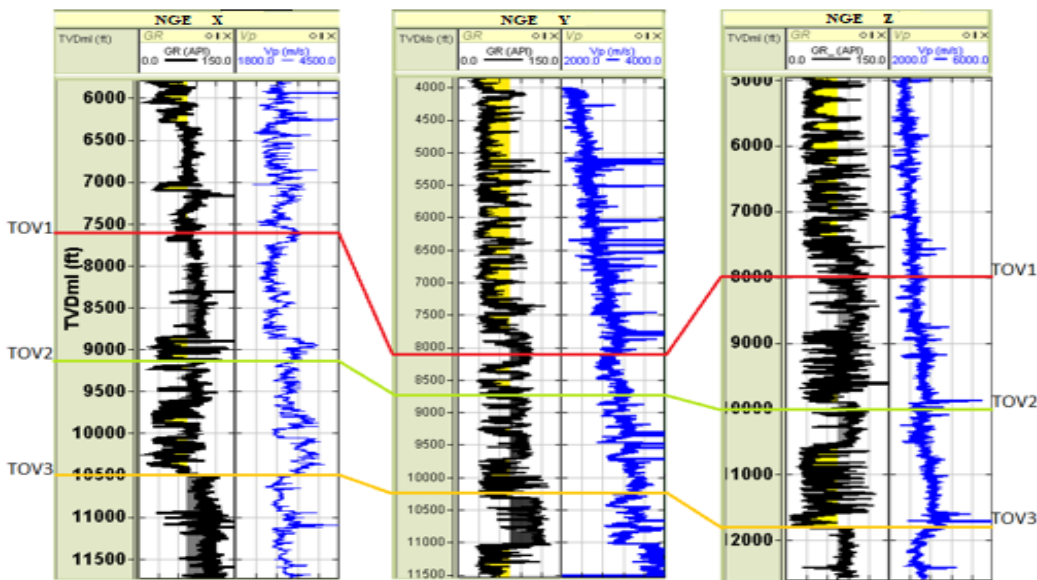


Figure 6. Correlation of Tops of overpressure in the studied wells (Nge X – Z)

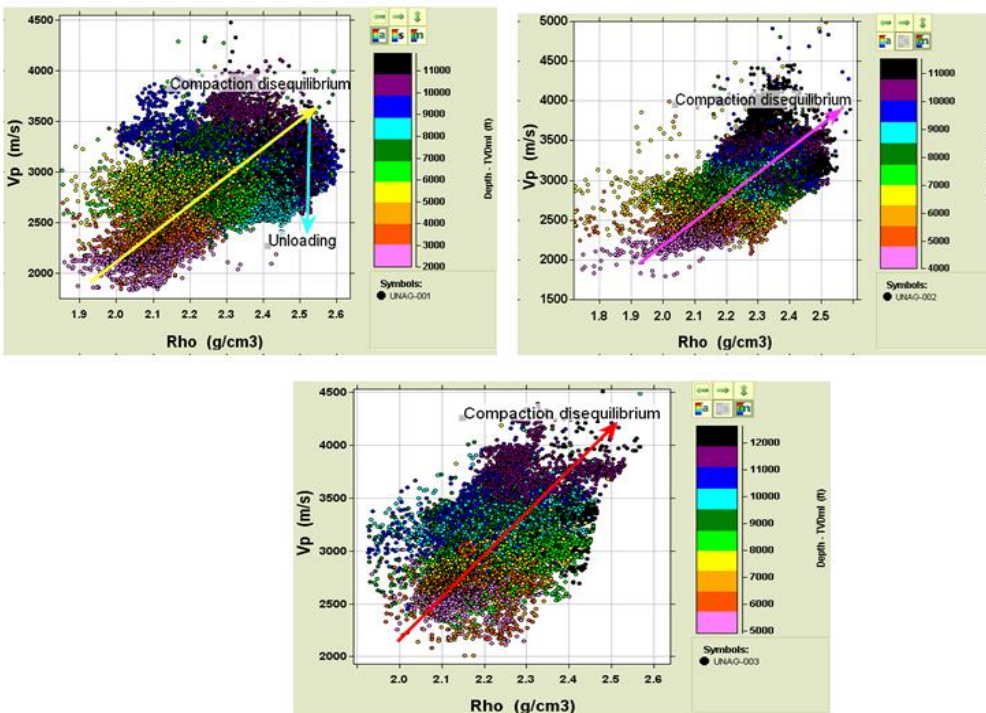


Fig. 7 cross plot of compressional velocity against density for NGE X – Z wells, (a) NGE X, (b) NGE Y, (c) NGE Z (Rokdoc software, 2010 version).

SUMMARY OF FINDINGS

The results of the effective stress/pressure cell method corresponded to a reduction in shale density and a decrease in effective stress of the entire formation as depth increases, indicating the presence of overpressure. Three distinct overpressure zones—A, B, and C—were identified across the wells in the NGE Field. The field exhibits mild overpressures attributed to under-compaction within depths ranging from 4,000ft to 10,200ft (overpressure zones A and B). Specifically, overpressure estimates for Zone A in well NGE X range from 4121.6psi to 5540.5psi, while Zone B shows similar characteristics. In contrast, hard overpressure was encountered between 10,500ft and 12,700ft (overpressure zone C), primarily due to unloading mechanisms observed in NGE wells X and Z. For instance, at a depth of 10,500ft, the measured pore pressure reached 5540.5psi, resulting in an overpressure of 994psi when compared to the normal pore pressure of 4546.5psi calculated using a normal pressure gradient of 0.433psi/ft. This study highlights the critical relationship

between pore pressure and rock integrity, suggesting that the unloading mechanism of overpressure is initiated under extreme conditions of under-compaction when pore pressure does not exceed the threshold necessary to fracture rock grains. As pressure accumulates with increasing depth, it can reach levels sufficient to support the entire weight of the overburden—a characteristic indicative of unloading. The findings suggest that the onset of unloading mechanisms is contingent upon specific geological conditions, particularly the interplay between pore pressure and rock strength. Comparative analysis with previous studies reinforces these findings. For example, Nfor and Ndicho (2011) identified overpressure zones in the X-field at approximately 7,000ft, revealing deviations in porosity indicative of abnormal pressures. Goodwyne (2012) also demonstrated the effectiveness of density logs for predicting overpressure, particularly in shallow sequences, aligning with the mild overpressure observed in zones A and B. Furthermore, Ugwu and Nwankwo (2014) noted that under-compaction was a primary mechanism in the Akata Shale, with pressure ranges from 0.71 psi/ft to 7.10 psi/ft at depths of 8,000ft to 13,000ft, supporting the findings of mild overpressure in the NGE Field.

Building on the findings presented, the identification and characterization of overpressure zones within the NGE Field have significant implications for future hydrocarbon exploration and drilling operations. Understanding the mechanisms that generate overpressure, such as disequilibrium compaction and unloading, allows for more accurate predictions of pressure regimes in subsurface formations. This knowledge is crucial for designing effective drilling programs that minimize the risks associated with overpressure, such as kicks and blowouts, which can lead to catastrophic incidents and substantial financial losses. By integrating seismic and well log data, operators can develop more reliable models for pore pressure prediction, enhancing safety and operational efficiency. In addition, the delineation of distinct overpressure zones A, B, and C provides valuable insights into the spatial distribution of pressure anomalies within the NGE Field. This information can guide drilling decisions, such as the selection of well locations and the implementation of appropriate drilling techniques tailored to the specific pressure conditions encountered. For instance, in areas identified with high overpressure, operators may consider using managed pressure drilling (MPD) techniques to maintain control over the wellbore and mitigate the risks associated with unexpected pressure fluctuations. In addition, the findings underscore the importance of continuous monitoring and reassessment of pressure conditions throughout the drilling process. As new data becomes available, operators should be prepared to adapt their strategies in response to evolving pressure dynamics. This proactive approach not only enhances safety but also optimizes resource extraction by ensuring that drilling operations are conducted in the most favourable conditions.

CONCLUSIONS

The insights gained from this study not only contribute to a deeper understanding of overpressure mechanisms in the Niger Delta but also provide a framework for improving exploration and drilling strategies. By leveraging advanced analytical techniques and integrating diverse data sources, the industry can enhance its ability to navigate the complexities of subsurface pressure regimes, ultimately leading to more successful and sustainable hydrocarbon exploration efforts.

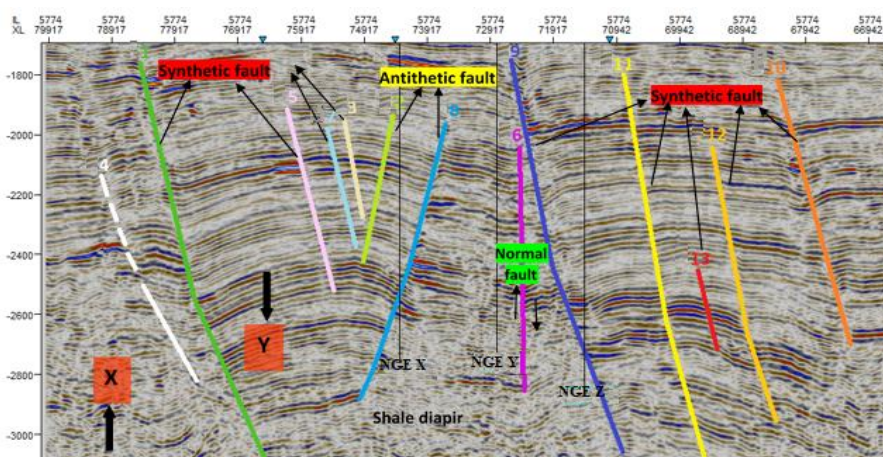


Figure 8 Interpreted seismic inline 5774 section (Petrel, 2016 version)

Table 3 Identified faults on seismic inline 5774.

Faults	Type of Fault	Direction of dip
F1	[Synthetic] Major growth fault	South
F2	[Antithetic] minor growth fault	West
F3	[Synthetic] minor growth fault	South
F4	[Synthetic] minor growth fault	South
F5	[Synthetic] minor growth fault	South
F6	[Antithetic] minor growth fault	South–west
F7	[Synthetic] minor growth fault	South
F8	[Antithetic] minor growth fault	West
F9	[Synthetic] Major growth fault	South
F10	[Synthetic] minor growth fault	South
F11	[Synthetic] Major growth fault	South
F12	[Synthetic] minor growth fault	South
F13	[Synthetic] minor growth fault	South

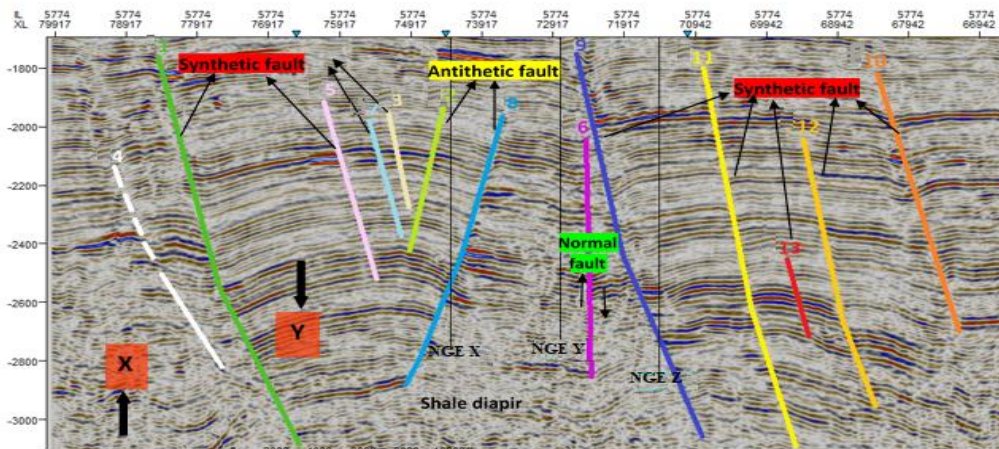
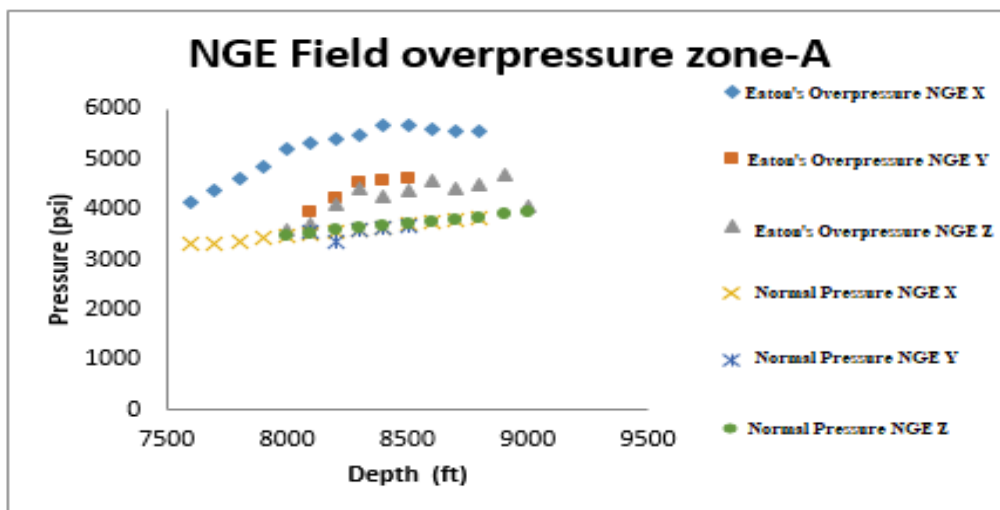


Fig. 9 Correlation of Tops of Overpressure (TOV) on seismic inline 5774 section (Petrel, 2016 version)



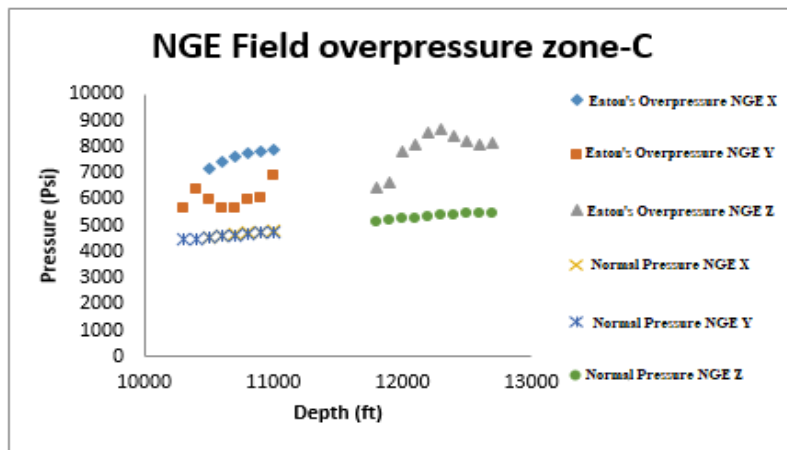
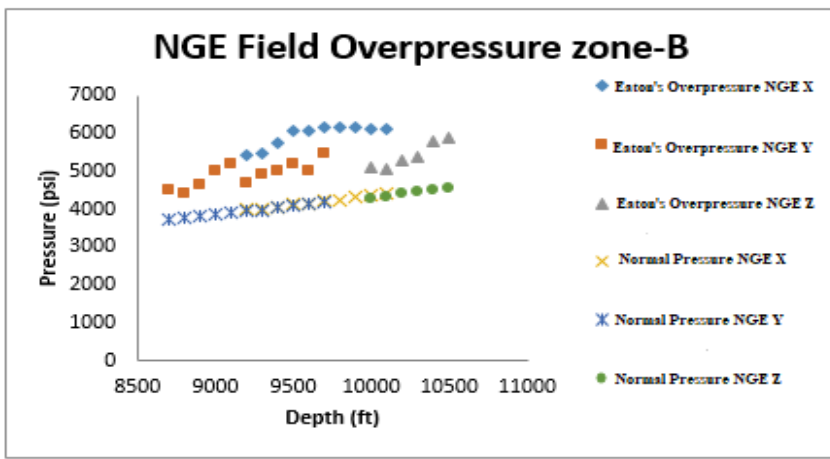
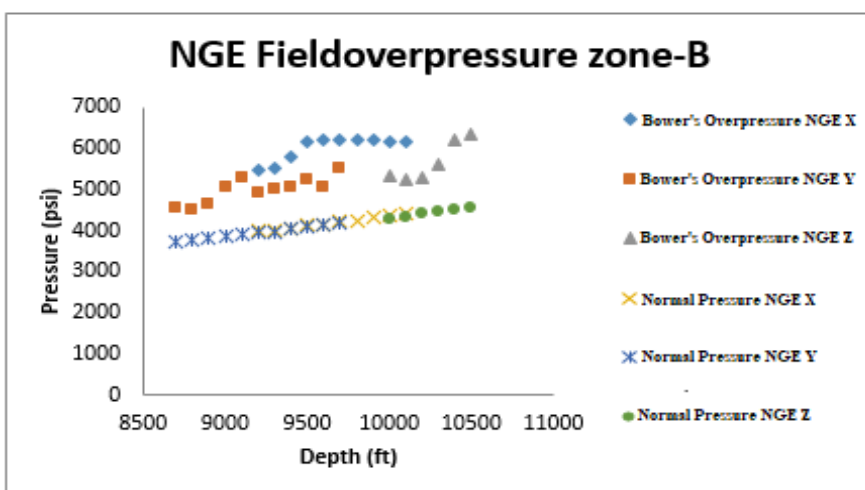
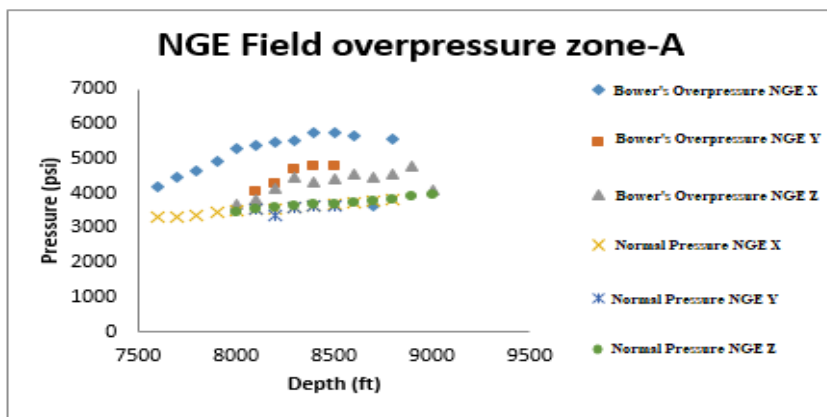


Fig 10 Overpressure zones cross-plots from Eaton's empirical model across the Study wells in NGE field



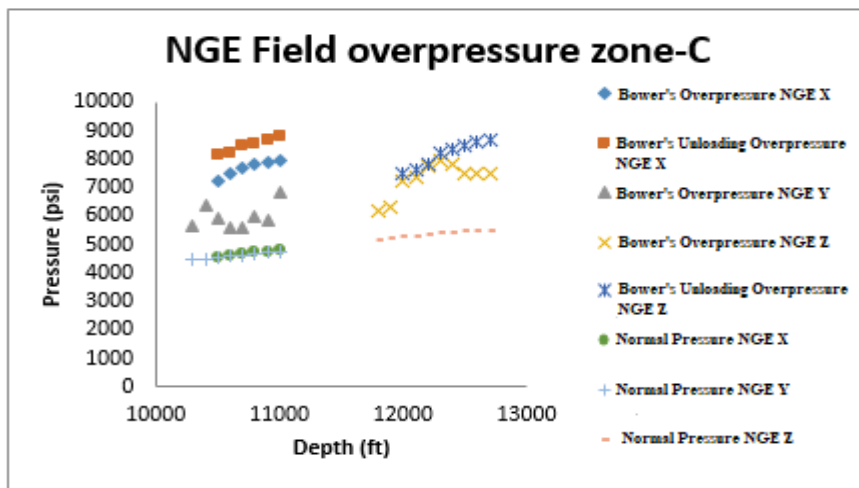


Fig 11 Overpressure zones cross-plots from Bowers empirical model across the Study wells in NGE field

REFERENCES

1. Abam, T. K. S., and Omuso, W. O. (2000). On river cross-sectional change in the Niger Delta. *Geomorphology*, 34(1-2), 111-126.
2. Abbey, C., Oniku, A., and Chukwudi Meludu, A. S. (2020). Rock physics analysis of abnormal pore pressure regime offshore Niger Delta Basin. *Jordan Journal of Earth and Environmental Sciences*, 11(3), 224-233.
3. Adegoke, O. S., Oyebamiji, A., Edet, J. J., Osterloff, P., and Ulu, O. K. (Eds.). (2016). *Cenozoic foraminifera and calcareous nannofossil biostratigraphy of the Niger Delta*. Elsevier.
4. Ahirakwem, C. A., and Opara, A. I. (2012). Application of Brine Concentrations as a Reconnaissance Geochemical Tool for Hydrocarbon Exploration: Case Study of Field "X", OML63, Coastal Swamp 1 Depobelt, Niger Delta Basin, Nigeria. *International Journal of Science and Technology*, 2(8), 507-516.
5. Ajakaiye, D. E., and Bally, A. W. (2002). *Course manual and atlas of structural styles on reflection profiles from the Niger Delta (Vol. 41)*. American Association of Petroleum Geologists.
6. Akpa, C., Nnabo, P. N., Ani, C. C., Obasi, A. I., Obasi, P. N., and Nworie, C. D. (2023). Application of ground magnetic method for delineation subsurface structural control on sulphide ore deposit in Benue Trough; A Case Study of Ikenyi Izzi. *Earth Sci Malays*, 7(1), 07-19.
7. Akrou, D., Ahmadi, R., Mercier, E., and Montacer, M. (2021). Present-day overpressure in southern Tunisia: Characterization, possible causes and implications for drilling operations. *Journal of African Earth Sciences*, 184, 104356.
8. Alao, O., Abegunrin, A., and Ofuyah, W. *Application of Well Log Data in Overpressure Identification—A Guide to Hydrocarbon Exploration Onshore Niger Delta*.
9. Alias, A. H. (2011). *Pore Pressure Estimation in HPHT Wells*.
10. Aminu, M. B., and Olorunniwo, M. O. (2012). Seismic paleo-geomorphic system of the extensional province of the Niger Delta: an example of the Okari field. *Tectonics-Recent Advances*.
11. Atashbari, V. (2016). *Origin of overpressure and pore pressure prediction in carbonate reservoirs of the Abadan Plain Basin (Doctoral dissertation)*.
12. Avbovbo, A. A. (1978). Tertiary lithostratigraphy of the Niger Delta. *Bulletin of the American Association of Petroleum Geologists*, 62(12), 2228-2236.
13. Barker, C. (1987). Development of abnormal and subnormal pressures in reservoirs containing bacterially generated gas. *AAPG bulletin*, 71(11), 1404-1413.
14. Birchall, T., Senger, K., and Swarbrick, R. (2022). Naturally occurring underpressure—a global review. *Petroleum Geoscience*, 28(2), petgeo2021-051.
15. Bjørlykke, K., and Høeg, K. (1997). Effects of burial diagenesis on stresses, compaction and fluid flow in sedimentary basins. *Marine and Petroleum Geology*, 14(3), 267-276.
16. Busari, M. O., and Adekeye, O. A. (2024). Impacts of structuration on slope channel geomorphology and internal architecture: a Pleistocene feeder channel-ponded lobe system, offshore Niger Delta. *Arabian Journal of Geosciences*, 17(6), 176.

17. Carvajal, O., and Sierra, C. (2020). Risk Mitigation in Overpressured Wells through Geomechanical Approach. In SPE Latin America and Caribbean Petroleum Engineering Conference (p. D041S039R002).
18. Chukwu, A., and Obiora, S. C. (2021). Petrogenesis and tectonomagmatic updates on the origin of the igneous rocks in the lower Benue rift, southeastern Nigeria. *Arabian Journal of Geosciences*, 14(3), 154.
19. De Souza, J. M. G. (2020). Modeling of overpressure evolution during the gravitational collapse of the Amazon deep-sea fan, Foz do Amazonas Basin (Doctoral dissertation, Sorbonne Université).
20. Dim, C. I. P., and Dim, C. I. P. (2021). Regional geology, basin forming tectonics and basin fills of Southern Benue Trough and Anambra Basin in Afikpo Area. *Facies Analysis and Interpretation in Southeastern Nigeria's Inland Basins*, 9-17.
21. Doust, H. (1990). *Petroleum geology of the Niger Delta*. Geological Society, London, Special Publications, 50(1), 365-365.
22. Eyinla, D. S., Oladunjoye, M. A., Olayinka, A. I., and Bate, B. B. (2021). Rock physics and geomechanical application in the interpretation of rock property trends for overpressure detection. *Journal of Petroleum Exploration and Production*, 11, 75-95.
23. Eze, S., Ideozu, R. U., Abel, I. T., Jacob, O. A., and Wasuu, O. O. (2018). Unloading Mechanism: An indication of Overpressure in niger Delta ('X'-Field) Using Cross Plots of Rock properties. *International Journal of Research in Social Sciences*, 8(3), 719-736.
24. Fertl, W. H. (1981). *Abnormal formation pressures*. Elsevier.
25. Ganguli, S. S., and Sen, S. (2020). Investigation of present-day in-situ stresses and pore pressure in the south Cambay Basin, western India: Implications for drilling, reservoir development and fault reactivation. *Marine and Petroleum Geology*, 118, 104422.
26. Godwin, E. O. (2013). Pore Pressure Prediction from Seismic Data in Part of the Onshore Niger Delta Sedimentary Basin. *Physics International*, 4(2), 152-159.
27. Goodwyne, O. (2012). *Pressure prediction and underbalanced drilling in the deepwater niger delta* (Doctoral dissertation, Durham University).
28. Gutierrez, M. A., Braunsdorf, N. R., and Couzens, B. A. (2006, October). Evaluation, calibration, and ranking of pore pressure prediction models. In *SEG International Exposition and Annual Meeting* (pp. SEG-2006). SEG.
29. Haack, R. C., Sundararaman, P., Diedjomahor, J. O., Xiao, H., Gant, N. J., May, E. D., and Kelsch, K. (2000). *AAPG Memoir 73, Chapter 16: Niger Delta Petroleum Systems, Nigeria*.
30. Hamid, M. (2013). *Pore Pressure Prediction in Shale Gas Field*.
31. Harrold, T. W. D. (2001). *Porosity and effective stress relationships in mudrocks* (Doctoral dissertation, Durham University).
32. Kogbe, C. A. (1976). *Geology of Nigeria*. Elizabethan Publishing Company.
33. Kogbe, C. A. (1978). The geology of the Niger Delta: Stratigraphy and structural evolution. *Bulletin of the American Association of Petroleum Geologists*, 62(4), 493-511.
34. Li, C., Zhan, L., and Lu, H. (2022). Mechanisms for overpressure development in marine sediments. *Journal of Marine Science and Engineering*, 10(4), 490.
35. Loudon, L. R. (1972, May). Origin and maintenance of abnormal pressures. In *SPE Abnormal Subsurface Pressure Symposium* (pp. SPE-3843). SPE.
36. Luo, X. R. (2004). Quantitative analysis on overpressuring mechanism resulted from tectonic stress. *Chinese Journal of Geophysics*, 47(6), 1223-1232.
37. Mavatikua, L. (2005). *Dependence of sonic velocity on effective stress in fine-grained sediments* (Doctoral dissertation, Durham University).
38. Nfor, B., and Ndicho, O. M. I. (2011). Porosity as an overpressure zone indicator in an X-field of the Niger Delta Basin, Nigeria. *Archives of Applied Science Research*, 3(3), 29-36.
39. Nwajide, C. S. (1990). The geology of the Ogwashi-Asaba Formation in Southeastern Nigeria. *Journal of African Earth Sciences*, 10(1), 143-150.
40. Nwonodi, R. I., and Dosunmu, A. (2021). Analysis of a porosity-based pore pressure model derived from the effective vertical stress. *Journal of Petroleum Science and Engineering*, 204, 108727.
41. Obaje, N. G. (2009). *Geology and mineral resources of Nigeria*. Springer.
42. Obaje, N. G., and Amajor, L. C. (2000). Oligocene-Miocene transition in the Benin Formation, Niger

- Delta Basin. *Nigerian Journal of Mining and Geology*, 36(1), 45-56.
43. Odesa, G. E., Ozulu, G. U., Eyankware, M. O., Mba-Otike, M. N., and Okudibie, E. J. (2024). A holistic review of three-decade oil spillage across the Niger Delta Region, with emphasis on its impact on soil and water. *World Scientific News*. WSN 190(2) (2024) 119-139. EISSN 2392-2192
 44. Ogbamikhumi, A., and Igbini, N. S. (2020). Rock physics attribute analysis for hydrocarbon prospectivity in the Eva field onshore Niger Delta Basin. *Journal of Petroleum Exploration and Production Technology*, 10, 3127-3138.
 45. Ojo, J. A., and Rahaman, M. A. (1989). The stratigraphy and Pleistocene deposits of the Benin Formation in the Niger Delta. *Geological Magazine*, 126(5), 527-535.
 46. Oloruntobi, O. S. (2019). The pore pressure, bulk density and lithology prediction (Doctoral dissertation, Memorial University of Newfoundland).
 47. Ovwigho, E. M., Almomen, M. S., Corona, M., and Terrez, J. (2023). Well Integrity Challenges while Drilling in High Pressure and Narrow Window Environment: A Case Study of a Deep Gas Field in the Middle East. In *SPE Middle East Oil and Gas Show and Conference* (p. D021S051R003).
 48. Petters, S. W. (1982). Stratigraphy and paleogeography of the Niger Delta. *AAPG Bulletin*, 66(6), 1016-1031.
 49. Rezaee, R. (Ed.). (2015). *Fundamentals of gas shale reservoirs*. John Wiley and Sons.
 50. Short, K. C., and Stauble, A. J., (1967): *Outline of Geology of Niger Delta: American Association of Petroleum Geologists, Bulletin, Vol. 51, pp. 761-779.*
 51. Suppe, J. (2014). Fluid overpressures and strength of the sedimentary upper crust. *Journal of Structural Geology*, 69, 481-492.
 52. Swarbrick, R. E., and Osborne, M. J. (1998). *Memoir 70, Chapter 2: Mechanisms that generate abnormal pressures: An overview.*
 53. Ugwu, S. A., and Nwankwo, C. N. (2014). Integrated approach to geopressure detection in the X-field, Onshore Niger Delta. *Journal of Petroleum Exploration and Production Technology*, 4, 215-231.
 54. Unuagba, T., Ideozu, R. U., Eze, S., Osung, E., and Abolarin, O. (2021). Prediction of Overpressure using Effective Stress and Velocity Trend Methods in Unag field Offshore Niger Delta. *International Journal of Research and Innovation in Applied Sciences*, 6(1), 134-145.
 55. Wright, J. B. (1985). The Benue Trough and coastal basins. *Geology and mineral resources of West Africa*, 98-113.
 56. Zhang, J., Wu, S., Hu, G., Yue, D., Xu, Z., Chen, C., Ke, Z. Junjie, W.. and Wen, S. (2021). Role of shale deformation in the structural development of a deepwater gravitational system in the Niger Delta. *Tectonics*, 40(5), e2020TC006491.
 57. Zhang, Y., Lv, D., Wang, Y., Liu, H., Song, G., and Gao, J. (2020). Geological characteristics and abnormal pore pressure prediction in shale oil formations of the Dongying depression, China. *Energy Science and Engineering*, 8(6), 1962-1979.